Depletion-Driven Phase Separation and Reversible Aggregation in Confined Colloidal Mixtures

E. K. Hobbie

National Institute of Standards and Technology, Gaithersburg, Maryland 20899

Received April 6, 1999. In Final Form: July 14, 1999

The kinetics of size segregation in quasi-two-dimensional binary mixtures of nearly-hard-sphere colloids were studied with video microscopy. During the transient fluid-fluid phase separation that occurs as an intermediate step in the formation of isolated large-sphere crystallites, the structure factor of the (larger) minority component exhibits a spinodal-like evolution, while the cluster-size distribution exhibits scaling reminiscent of colloidal aggregation. The scaled distributions suggest a crossover from power-law ($x < 1$) to stretched-exponential ($x > 1$) behavior, where $x = k/s$ is the ratio of the cluster-size index to the average cluster size. A phenomenological explanation based on the reversible Smoluchowski equation is proposed.

I. Introduction

Colloidal aggregation can bear a striking resemblance to phase separation in binary fluid mixtures.[1] While the former is typically associated with the flocculation of particles and particle clusters inherently far from equilibrium, the latter is typically associated with the time evolution of thermodynamically unstable or metastable states and the kinetics of partitioning between coexisting phases.[2] The segregation of a binary fluid[2] and the crystallization of a simple liquid[3] are by themselves familiar examples of first-order phase transitions; however, these two phenomena can be driven simultaneously, for example, in mixtures whose components interact predominantly through excluded volume via a so-called depletion force.[4,5] In a recent study of depletion-driven self-assembly in gravitationally confined nearly-hard-sphere mixtures,[6] the crystallization of the minority component was observed to occur via a two-stage process governed by an initial collapse into an amorphous metastable state, in a manner reminiscent of behavior observed in colloid/polymer mixtures.[7,8] The growth kinetics associated with the formation of these transient states might offer a novel glimpse into the earliest stages of segregation in a model binary mixture, further elucidating similarities that exist between conventional colloidal aggregation and the well studied processes of spinodal decomposition and nucleation.

Here, the kinetics of depletion-driven size segregation were studied with video microscopy in a quasi-two-dimensional system as the mixtures collapse into a dense metastable "fluid" state after shear melting. During this initial fluid-fluid phase separation, the structure factor of the minority component exhibits a spinodal-like evolution while the cluster-size distribution exhibits scaling reminiscent of colloidal aggregation. The data suggest that scaled distributions show a crossover from power-law ($x < 1$) to stretched-exponential ($x > 1$) behavior, where $x = k/s(t)$ is the ratio of the cluster-size index, k, to the time-dependent average cluster size, $s(t)$, where "size" denotes number of particles. By varying the small-sphere volume fraction, a variety of quench depths were considered, and a phenomenological model based on the reversible form of the Smoluchowski equation is presented. The paper gives a more detailed description of the work described in ref 6. The colloidal particles used in this study are smaller and more mobile than those used in a previous study,[9] and hence a larger and more significant range of cluster sizes is achieved.

II. Experimental Background

The mixtures consisted of monodisperse ($\sigma_R/R \sim 0.035$, where σ_R is the width of the radius-distribution function) polystyrene spheres (stabilized with a charged polymer surfactant) of diameter $2R_L = 2.9\ \mu$m (obtained from Polysciences) and $2R_S =$ 213 nm (obtained from Seradyn) in aqueous suspensions containing enough salt (0.01 M) to screen the electrostatic repulsion to short range. The large-sphere volume fraction was fixed at $\phi_L = 0.025$ for small-sphere volume fractions $0 \le \phi_S \le 0.40$, where (relative) volume fractions were obtained from the measured change in mass of small amounts of sample after drying in a vacuum oven. Quoted small sphere volume fractions had an uncertainty of ± 0.01. Large-sphere suspensions ($\phi_L = 0.025$) were separated in a centrifuge, and the solvent was drawn off and replaced with an equal volume of filtered small-sphere suspension ($\phi_S = 0.30$) to get stock ($\phi_S = 0.30$, $\phi_L = 0.025$) mixtures. Mixtures with $\phi_S < 0.30$ were then obtained by diluting these stock suspensions with $\phi_L = 0.025$ solutions (0.01 M NaCl in purified water). Small-sphere volume fractions of 0.40 were obtained via separation of the $\phi_S = 0.30$ suspensions in a centrifuge. A measured amount of pure solvent was then drawn off, after which the samples were redispersed and briefly returned to the centrifuge to remove flocs. Clean $\phi_S = 0.40$ suspension was then drawn from the top of the sample and checked under the microscope for purity. Mixing with the large spheres proceeded in the same manner as for $\phi_S = 0.30$ suspensions.

As in a previous study,[9] gravitational settling of the large spheres restricts their motion to a plane, with the confinement axis parallel to the optical axis of the microscope, which leads

(1) (a) Robinson, D. J.; Earnshaw, J. C. *Phys. Rev. Lett.* **1993**, *71*, 715. (b) Carpineti, M.; Giglio, M. *Phys. Rev. Lett.* **1993**, *70*, 3828. (c) Carpineti, M.; Giglio, M. *Phys. Rev. Lett.* **1992**, *68*, 3327.

(2) See, for example: Gunton, J. D.; San Miguel, M.; Sahni, P. S. In *Phase Transitions and Critical Phenomena*; Domb, C., Lebowitz, J. L., Eds.; Academic: London, 1983; Vol. 8.

(3) Chaikin, P. M.; Lubensky, T. C. *Principles of Condensed Matter Physics*; Cambridge University Press: Cambridge, 1995.

(4) Asakura, S.; Oosawa, F. *J. Chem. Phys.* **1954**, *22*, 1255.

(5) See, for example: (a) Dinsmore, A. D.; Yodh, A. G.; Pine, D. J. *Phys. Rev. E* **1995**, *52*, 4045. (b) Dijkstra, M.; van Roij, R.; Evans, R. *Phys. Rev. E* **1999**, *59*, 5744.

(6) Hobbie, E. K. *Phys. Rev. Lett.* **1998**, *81*, 3996.

(7) See, for example: Poon, W. C. K.; Pirie, A. D.; Pusey, P. N. *Faraday Discuss.* **1995**, *101*, 65 and references therein.

(8) See, for example: Soga, K. G.; Melrose, J. R.; Ball, R. C. *J. Chem. Phys.* **1999**, *110*, 2280 and references therein.

(9) (a) Hobbie, E. K. *Phys. Rev. E* **1997**, *55*, 6281. (b) Hobbie, E. K.; Holter, M. J. *J. Chem. Phys.* **1998**, *108*, 2618.

10.1021/la990397o CCC: $18.00
Published on Web 10/07/1999

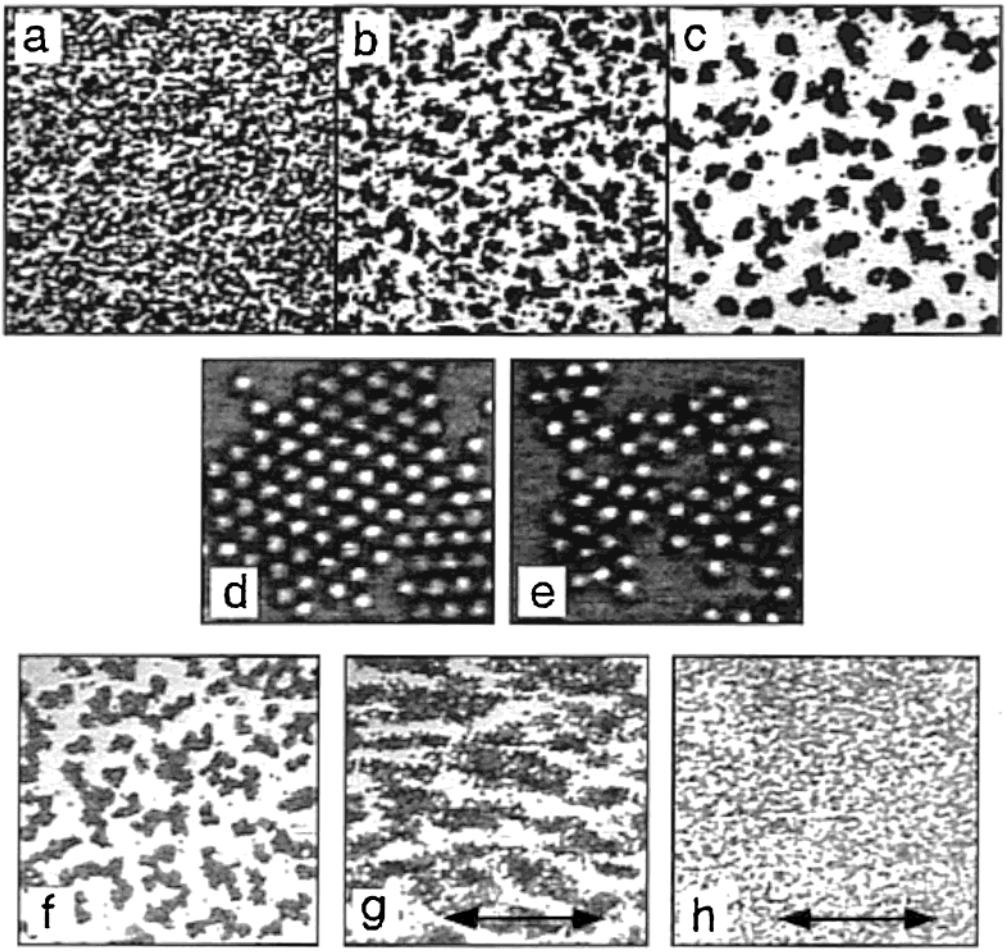

Figure 1. Coarse-grained structure for $\phi_S = 0.25$ at (a) 2 min, (b) 60 min, and (c) 20 h after shear melting. The width of each micrograph is 350 μm. Typical packing morphology at $t = 15$ h: (d) $\phi_S = 0.20$; (e) $\phi_S = 0.30$, where the width of each micrograph is 30 μm. Phase-separated domains (f) are easily deformed [(*g*) $t = 2$ s after imposition of flow] and sheared apart [(*h*) $t = 120$ s after imposition of flow] by oscillatory shear flow ($f = 1$ Hz with an amplitude such that single large spheres are displaced $20R_L$ in one cycle) in the direction indicated by the arrows.

to approximately two-dimensional trajectories on the surface of a smooth glass substrate. This facilitates tracking of the large spheres and gives rise to an effective conservation law associated with the large-sphere number. Qualitatively, a spherical shell of volume (thickness R_S) surrounds each large sphere, from which the center of each small sphere is excluded. This implies that when two large spheres come into contact, the effective value of ϕ_S decreases, thereby lowering the entropic free energy by an amount Δ.[4] If Δ/k_BT is large enough, the large spheres aggregate into clusters. For the confined geometry of interest, a close-packed triangular lattice yields the greatest reduction in excluded volume and hence the greatest decrease in free energy. The value of ϕ_L used in this study is below the percolation threshold, and phase separation was only observed for $\phi_S \geq 0.20$, in qualitative agreement with the bulk phase diagram reported by Dinsmore et al.[5] for a comparable system in three dimensions.

The sample cell was an epoxy-sealed microscope slide and cover slip with a 15-μm thermocouple wire as spacer. Capillary pressure wicks the suspension into the cell, which has two small openings at either end; the cell is then dried and completely sealed with fast curing epoxy. All of the measurements were carried out at an ambient temperature of (22 ± 0.5) °C. Digitized video micrographs were collected with both 10× and 40× objectives to obtain coarse- and fine-grained images (frame width $\approx 10^3$ μm and 200 μm, respectively) of the evolving domain structure during phase separation and subsequent crystallization (Figure 1). The latter yields just over 10^3 large-sphere centers per video frame, and data from around 15 frames were averaged together for a typical measurement. This was accomplished by recording the relaxation after repeated shear melting (Figure 1), where the shear flow was introduced by gently compressing the cover slip of the sample cell. Frames taken with the 40× objective were digitized and computer-analyzed to obtain the planar coordinates of the large-sphere centers (±100 nm). Frames taken with the 10× objective were Fourier analyzed, averaged together, azimuthally averaged, and then divided by the analogous quantity for $\phi_S = 0$, which approximates dividing out the large-sphere form factor.

III. Experimental Results

The phase-separation kinetics were studied via the cluster-size distribution function, $n_k(t)$, and the structure factor, $S(q,t)$, of the minority large-sphere component. The radial-distribution function, $g(r)$, exhibits a nearest-neighbor peak at $2R_L$ [Figure 2a], the width of which yields a criterion for clustering.[10] The distribution $n_k(t)$ gives the probability of finding a large sphere in a cluster of size k at time t subject to the constraint

$$\sum_k k n_k(t) = 1$$

imposed by particle conservation, where the largest clusters observed typically contained on the order of 10^2

(10) The clustering criterion is set as an input parameter in the computer code that tabulates n_k from the large-sphere centers and was chosen as the distance at which $g(r)$ decays to 0.75 of its nearest-neighbor value. Slight deviations from this did not significantly alter the results, and the same criterion was used for all ϕ_S. Distributions from different frames corresponding to the same time were normalized and then averaged together.

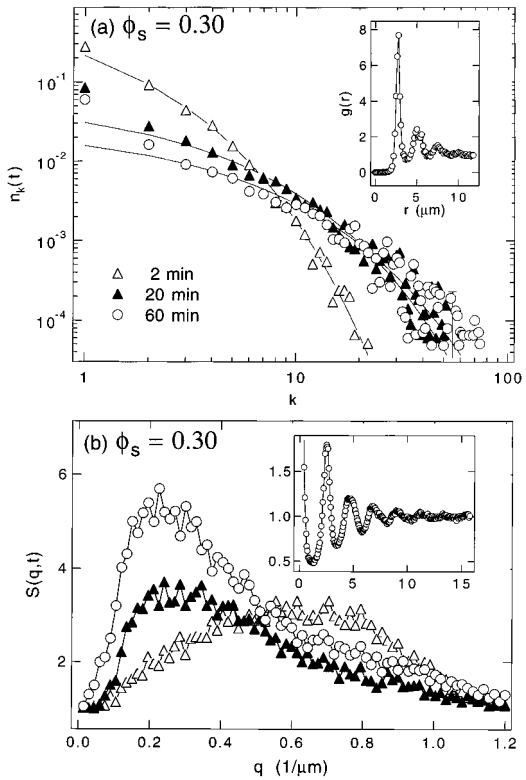

Figure 2. (a) $n_k(t)$ and (b) $S(q,t)$ for $\phi_S = 0.30$ during the first hour of phase separation, where the markers correspond to the times after shear melting shown in the top figure. The inset in (a) shows $g(r)$ at $t = 60$ min, and the large-k fits of $n_k(t)$ are as described in the text, with $\nu \approx 0.6$. The lower figure shows the time evolution of the low-q peak in $S(q,t)$, and the inset shows the higher-order structure in $S(q,t)$ at $t = 60$ min.

large spheres. $S(q,t)$ has higher-order peaks at fixed $q > 1\ \mu m^{-1}$ whose intensities increase with time and a spinodal-like peak at $q_m(t) < 1\ \mu m^{-1}$ that moves toward lower q and increases in intensity with time, reflecting an average cluster diameter $R(t) \sim 2\pi/q_m(t)$. Examples of $n_k(t)$ and $S(q,t)$ for $\phi_S = 0.30$ are shown in Figure 2.

Figure 3a shows how the higher-order structure evolves from $\phi_S = 0$ to $\phi_S = 0.20$. For $\phi_S < 0.20$, no phase separation was observed. Rather, this regime was characterized by transient clustering consistent with a weak short-ranged attraction, and structures that formed always eventually broke apart due to thermal fluctuations. The structure factor and cluster-size distribution for small-sphere volume fractions within this *miscible* region of the phase diagram were independent of time, in contrast to the time evolution shown in Figure 3b for a shear quench at $\phi_S = 0.30$. As shown in Figure 3a, the position of the nearest-neighbor peak at q_o ($\sim 2\pi/R_L$) gradually evolves toward slightly higher q with increasing small-sphere volume fraction, suggesting that the strength of the weak attraction increases slightly as the phase boundary is approached.

The aggregation is reversible, and phase-separating mixtures initially reach a state of cluster/single-particle coexistence. The amorphous clustering leads to a liquidlike structure factor (Figures 3−4) with a nearest-neighbor peak at $q_o \approx 2.5\ \mu m^{-1} \approx 2\pi/\sqrt{3}R_L$, while $n_k(t)$ is described by $n_k(t) = n_o(t)\exp[-\alpha(t)k^\nu]$ at large k with $\nu = 0.55-0.60$ for all ϕ_S [Figure 2a]. After an intermediate period of metastability, the aggregates start to collapse into an ordered solid.[6] Fragmentation becomes less common, and $n_k(t)$ becomes weighted toward larger k as the crystalline domains coarsen. The sequence from shear-melted fluid

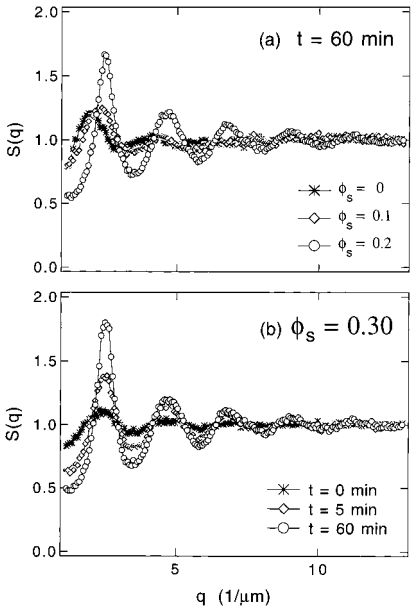

Figure 3. (a) Higher-order structure in $S(q,t)$ at $t = 60$ min for $\phi_S = 0$, 0.10, and 0.20. The structure for $\phi_S = 0$ and 0.10 is independent of time, while that for $\phi_S = 0.20$ evolves with time after shear melting, reflecting macroscopic phase separation, as shown in (b) for $\phi_S = 0.30$.

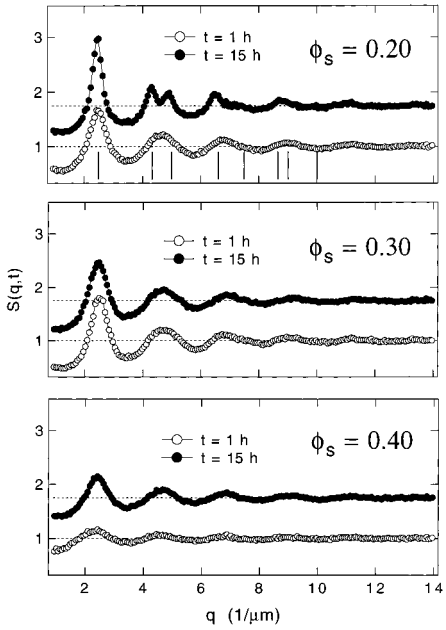

Figure 4. Late-time evolution of $S(q,t)$ for $\phi_S = 0.20$, 0.30, and 0.40. The vertical bars show the first eight Bragg peaks for a two-dimensional close-packed crystal with $2R_L = 2.9\ \mu m$. The curves for $t = 15$ h have been offset by 0.75 for clarity.

to isolated large-sphere crystallites is shown in Figure 1a−c. Crystalline ordering is evident as an increase in the intensity of the principal Bragg peak as well as a splitting of the second-order peak, as shown in Figure 4. For deep quenches ($\phi_S \geq 0.30$), the samples do not crystallize over the course of the experiment, and for $\phi_S = 0.40$, the aggregation process is greatly slowed.

The viscosity of the host small-sphere suspension increases with increasing ϕ_S, and it is convenient to work with the reduced time t/τ, where $\tau = 2dR_L^2\triangle t/\langle|\triangle\mathbf{r}|^2\rangle$ is a characteristic diffusion time of an isolated large sphere. In this expression, $\langle|\triangle\mathbf{r}|^2\rangle$ is an ensemble average of the mean-square displacement of a single large sphere during an interval of time $\triangle t$, which was chosen to be 60 s for the

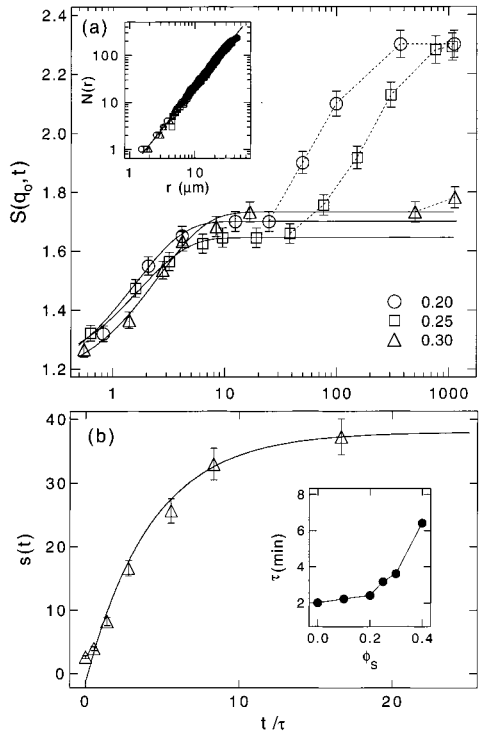

Figure 5. (a) $S(q_o,t)$ versus t/τ, where the fits up to the first plateau are as described in the text. The inset shows $N(r)$ vs r at $t/\tau \sim 20$ for some of the larger clusters. (b) Average cluster size, $s(t)$, vs t/τ for $\phi_S = 0.30$ during the first hour of phase separation, where the fit is as described in the text. The inset shows $\tau(\phi_S)$.

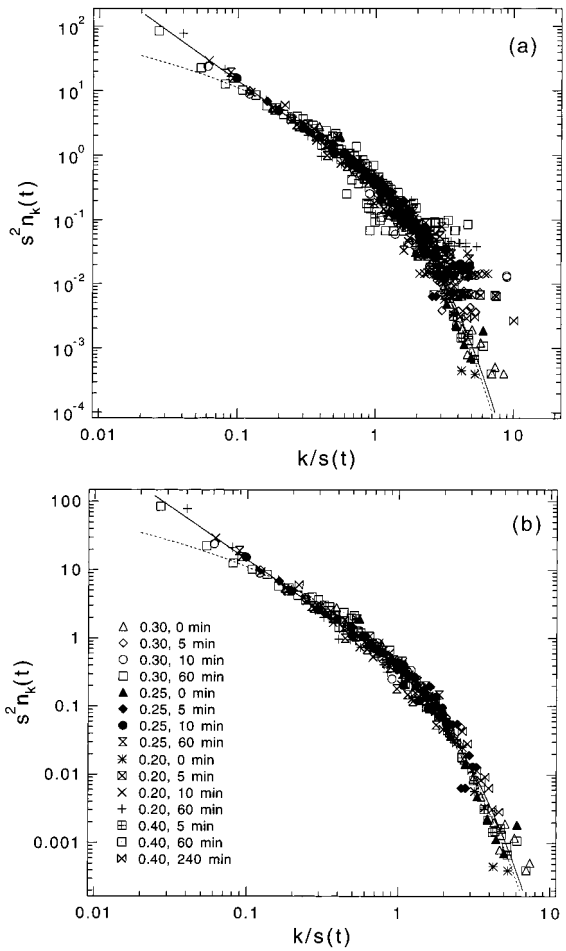

Figure 6. (a) $s^2n_k(t)$ vs $x = k/s(t)$ in the regime of amorphous growth, where the dashed curve is a large-x fit of the data, the solid line is a power law that describes the data for $x < 1$, and the solid curve is a stretched-exponential decay that describes the data for $x > 1$, as outlined in the text. (b) The same plot as (a) but with the distributions truncated at $k = 20$ to eliminate scatter in the data at large k.

mixtures described here, and $d = 2$ for the confined samples under consideration. A plot of $\tau(\phi_S)$ is shown in the inset to Figure 5b. Two quantities of fundamental interest are the intensity of the principal Bragg peak, $S(q_o,t)$, and the mass-averaged average cluster size

$$s(t) = \sum_k k^2 n_k(t)$$

Examples of the relaxation of these two quantities are shown as a function of t/τ in Figure 5. The two-stage nature of the crystallization process[6] is readily seen by following the time evolution of $S(q_o,t)$ [Figure 5a], where the mixtures reach an initial plateau before starting to order.[11] The morphology (Figure 1) of the intermediate (metastable) phase suggests fractal-like structures, and some of the larger clusters at different ϕ_S were analyzed by calculating $N(r)$, the number of monomers as function of the radial distance from the cluster center of mass. The inset to Figure 5a shows a log−log plot of the average $N(r)$ versus r for large clusters at different ϕ_S. The curves fall onto a power law of the form $N(r) \sim r^D$ with $D \approx 1.7$, reflecting the slightly open and disordered packing of the amorphous clusters.

Figure 5b shows the time evolution of $s(t)$ for $\phi_S = 0.30$ during the first hour of phase separation, which corresponds to the evolution of $S(q_o,t)$ up to the first plateau in Figure 5a. Similar behavior was observed for all ϕ_S from 0.20 to 0.30, but $\phi_S = 0.40$ exhibited phase separation on a much slower time-scale that was limited to smaller cluster growth.[6,11] The fit of $s(t)$, as well as the fit of $S(q_o,t)$ during the growth of the metastable phase, is an exponential relaxation of the form $\delta\psi(t) = \delta\psi_o \exp(-a_\psi t/\tau)$, where $\delta\psi(t) = \psi_m - \psi(t)$ is the displacement of the relevant quantity [$\psi(t) = s(t)$, $S(q_o,t)$] from its metastable value (ψ_m). Other quantities that provide a somewhat coarser measure of the phase separation, such as the probability of finding a large sphere in a cluster and the average domain diameter $R(t) = 2\pi/q_m(t)$, can also be described by an exponential relaxation of this form, and all of these show a dramatic decrease in both a_ψ and ψ_m for $\phi_S > 0.30$.[6]

Starting from the reversible form of the Smoluchowski equation with the assumptions of scaling[12] and kernel homogeneity, Sorensen et al.[13] have shown that coagulation/fragmentation systems can exhibit steady-state distributions to which $s(t)$ relaxes exponentially. With an ensemble of around 1.5×10^4 particles, there is scatter in $n_k(t)$ at large k [see error bar, Figure 2a]. Within this uncertainty, $n_k(t)$, indeed, appears to scale as $s^2n_k(t) = G(k/s)$ [Figure 6a], where s typically varies from around

(11) Crystallization becomes suppressed for $\phi_S \geq 0.3$, suggesting that the system becomes trapped in the amorphous phase. For $\phi_S = 0.40$, mixtures exhibit phase separation on a much slower time-scale, with an initial plateau at $t = 10$ h with $S(q_o,t) \sim 1.4$ that eventually progresses to $S(q_o,t) \sim 1.5$ after 2 days.

(12) (a) Family, F.; Meakin, P.; Deutch, J. M. *Phys. Rev. Lett.* **1986**, *57*, 727. (b) Family, F.; Meakin, P.; Deutch, J. M. *Phys. Rev. Lett.* **1986**, *57*, 2332. (E). Corrections to this scaling ansatz have been demonstrated [(c) Meakin, P.; Ernst, M. H. *Phys. Rev. Lett.* **1988**, *60*, 2503, and (d) Vigil, R. D.; Ziff, R. M. *Phys. Rev. Lett.* **1988**, *61*, 1431], but these corrections can be relatively small [(e) Elminyawi, I. M.; Gangopadhyay, S.; Sorensen, C. M. *J. Colloid Interface Sci.* **1991**, *144*, 315].

(13) Sorensen, C. M.; Zhang, H. X.; Taylor, T. W. *Phys. Rev. Lett.* **1987**, *59*, 363.

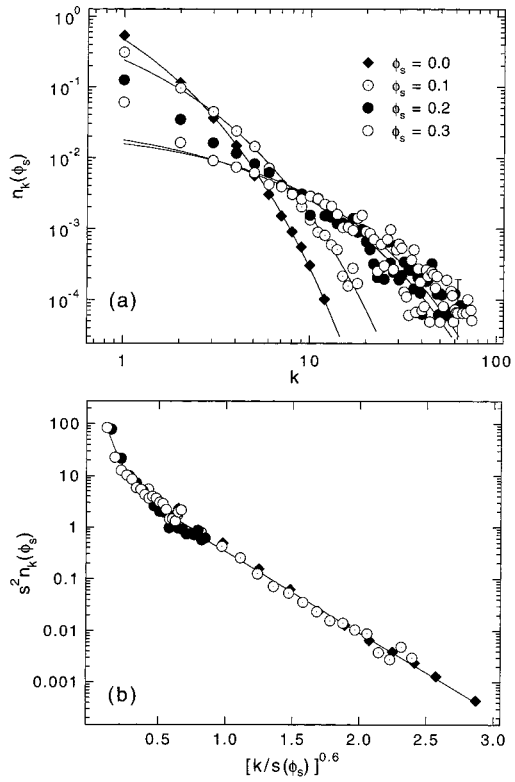

Figure 7. (a) Steady-state cluster-size distribution for different small-sphere volume fractions, where the data for $\phi_S = 0.20$ and 0.30 correspond to $t = 60$ min after shear melting, and the fits are as described in the text. The data for $\phi_S = 0$ and 0.10 are independent of time and reflect the presence of transient liquidlike clustering. (b) Semilogarithmic plot of the scaled cluster-size distribution, $s^2 n_k(\phi_S)$ vs $x^{0.6}$, where $x = k/s$ and the distributions have again been truncated at $k = 20$. The asymptotic fits are $x^{-1.45}$ for $x < 0.8$ and $\exp(-3.6x^{0.6})$ for $x > 0.8$.

2 at $t = 0$ to around 30 in the first plateau of $S(q_o,t)$. Some of the scatter inherent to this type of scaling plot can be eliminated by truncating the distributions[14] at $k = 20$, as shown in Figure 6b. The asymptotic fits (solid curves) of the scaled data in Figure 6 are $G(x) \sim x^{-1.53}$ for $0 < x < 1$ and $G(x) \sim \exp(-3.5x^{0.6})$ for $1 < x < \infty$.[15] A power law for $x \rightarrow 0$ is reminiscent of reaction-limited aggregation,[16] which is interesting, as the particles do not necessarily bond upon contact when the aggregation is reversible. An exponential decay has been suggested for large x,[17] and we cannot rule out the possibility that the actual behavior is in fact something more complicated, such as a power-law times an exponential decay that happens to be well approximated by a stretched exponential decay over the range of x in question. The data presented here suggest that a stretched-exponential decay might give an appropriate description, and thus a possible explanation for this is given in the following section.

Figure 7a shows n_k versus k as a function of ϕ_S, where the distributions for $\phi_S \geq 0.20$ again correspond to the first plateau in Figure 5a, or roughly 1 h after shear melting, while those for $\phi_S < 0.20$ are independent of time and correspond to the continuous formation and breakup of small transient clusters. The asymptotic large-k fits are again stretched exponential, with a stretching exponent (ν) that varies from $\nu \approx 0.50$ for $\phi_S < 0.20$ to $\nu \approx 0.60$ for $\phi_S > 0.20$. As shown in Figure 7b, the distributions appear to exhibit the same scaling exhibited by the distributions in Figure 6, with the asymptotic fits $x^{-1.45}$ ($x < 0.8$) and $\exp(-3.6x^{0.6})$ ($x > 0.8$). As before, the distributions have been truncated at $k = 20$ to eliminate scatter in $n_k(\phi_S)$ at large k, and the data are plotted semilogarithmically as a function of $[k/s(\phi_S)]^{0.6}$ to emphasize the stretched-exponential-like quality at large k; however, it must be emphasized again that this may simply turn out to be an approximate representation of a more complicated expression.

IV. Phenomenological Model

In the theoretical approach adopted here, a description of the phase separation process up to and including the first plateau in Figure 5a starts with the reversible form of the Smoluchowski equation:

$$\dot{n}_k = \frac{1}{2}\sum_{i=1}^{k-1}(K_{i,k-i}n_i n_{k-i} - F_{i,k-i}n_k) - \sum_j (K_{kj}n_k n_j - F_{kj}n_{k+j}) \quad (1)$$

where K_{ij} and F_{ij} are coagulation and fragmentation kernels, respectively.[2] One can make general arguments based on eq 1 that, although far from rigorous, might offer insight into a more detailed theoretical description of the clustering observed in this type of quasi-two-dimensional phase-separation phenomena, and it is hoped that the description given here will help motivate such work. For $k \rightarrow \infty$, a dominant growth mechanism is the gain and loss of smaller clusters. Assuming a coagulation kernel of the form

$$K_{ki} = (a/\tau)(k^{1/D} + i^{1/D})^{D-1}(\gamma_k^2 + \gamma_i^2)^{1/2} \quad (2)$$

where $\gamma_i \rightarrow 0$ for large i,[18] the $k \rightarrow \infty$ limit gives $K_{ki} \sim i^y \gamma_i k^y$ with $y = 1 - 1/D$, somewhat reminiscent of Becker–Döring theory.[2] Equation 2 simply approximates the kernel as the product of a *ballistic* term, $(\gamma_k^2 + \gamma_i^2)^{1/2}$, that models the mobility of the clusters and is related to their root-mean-square velocities, and a *cross-sectional* term, $(k^{1/D} + i^{1/D})^{D-1}$, that models the increased probability for large clusters to be struck by smaller clusters due to their increased perimeter, where the "circumference" is assumed to scale as r^{D-1}. If the first plateau in Figure 5a is viewed as a transient steady state of eq 1, the condition of detailed balance[2] offers a relation between the two kernels and the metastable-fluid cluster-size distributions, denoted by $(n_k)_m$. Specifically, the fragmentation kernel can be written as

$$F_{kj} = K_{kj}(n_k)_m(n_j)_m/(n_{k+j})_m \quad (3)$$

(14) Although the distributions are truncated at $k = 20$ in Figure 6b, the values of $s(t)$ used to reduce the data are calculated from the entire distribution.

(15) Distributions tabulated by hand directly from the images exhibited the same behavior as those tabulated by computer. A visual clustering criterion is not precise, however, while the computer algorithm misses some large spheres due to contrast variations. As a consequence, the former is weighted toward larger k and yields slightly higher moments.

(16) (a) Broide, M. L.; Cohen, R. J. *Phys. Rev. Lett.* **1990**, *64*, 2026. (b) Weitz, D. A.; Lin, M. Y. *Phys. Rev. Lett.* **1986**, *57*, 2037.

(17) (a) Meakin, P.; Deutch, J. M. *J. Chem. Phys.* **1985**, *83*, 4086. (b) Elminyawi, I. M.; Gangopadhyay, S.; Sorensen, C. M. *J. Colloid Interface Sci.* **1991**, *144*, 315.

(18) For this kernel to be homogeneous requires that γ_i exhibit a power-law decay in i. As in a previous study,[9] the cluster center-of-mass diffusion coefficient decreases dramatically above a cutoff cluster size, which in the present study is around 10–20. Large ($k > 100$) clusters would typically only diffuse on the order of one large sphere diameter during a time interval on the order of several hours.

Substituting eq 3 into eq 1 and expanding terms of the form $f_{k\pm i}$ to leading order in a Taylor series (assuming $i \ll k$) as

$$f_{k\pm i} \approx f_k \pm i\frac{\partial f_k}{\partial k} + ... \tag{4}$$

we arrive at the following approximate partial-differential equation for $n_k(t)$, valid in the limit of large k:

$$\frac{\partial n_k(t)}{\partial t} \approx \Gamma(t)\frac{\partial}{\partial k}[k^y n_k(t)] + ... \tag{5}$$

where $y = 1 - 1/D$,

$$\Gamma(t) = (a/\tau)\sum_i i\gamma_i \delta n_i(t) \tag{6}$$

and

$$\delta n_i(t) = (n_i)_m - n_i(t) \tag{7}$$

In general, higher-order terms in eq 5 are not negligible, and eqs 1 and 5 for $n_i(t)$ and $n_k(t)$, respectively, are nonlinearly coupled. With $x = k/s$, the scaling relation $n(x,t) = s^{-2}G(x)$ implies that terms other than $\partial n/\partial t$ must scale as $\dot{s}/s$, and a *phenomenological* solution can be obtained by truncating the expansion to leading order in i/s and replacing $\Gamma(t)$ with $c\dot{s}/s$, where c is a constant. Equation 5 is then separable in x and t in a manner that is consistent with scaling and yields the ordinary differential equation

$$\frac{\mathrm{d}(x^y G)}{\mathrm{d}x} = -2\frac{G}{c} \tag{8}$$

with the solution

$$G(x) = G_o x^{-(1-1/D)} \exp(-2Dx^{1/D}/c) \tag{9}$$

A large-x fit to this expression ($c = 1.2$ and $G_o = 7$) is shown as a dashed curve in Figure 6 with $\nu = 1/D \approx 0.6$. For $x \to 0$, which is an inappropriate limit for the above arguments, eq 9 gives $x^{-0.4}$, which is significantly less than the observed exponent of around 1.5.

V. Conclusions

The scaling in Figure 6 suggests that changes in the kinetics with quench depth (ϕ_S) are contained in the moment $s(t)$, while the scaling form itself appears to be independent of quench depth. This is interesting, in light of the recent demonstration by Crocker et al.[19] that the hard-sphere liquid structure of the host small-sphere suspension gives rise to oscillations and barriers in the effective pair potential between adjacent large spheres. The scaling would seem to suggest that the complicated spatial structure of the depletion attraction, although coarsely limiting the equilibration rate through the coefficient $a_\psi(\phi_S)$, does not grossly affect the analytic form of the distribution $n_k(t)$. This is somewhat reminiscent of critical phenomena, where the details of the molecular interaction are irrelevant to the details of the universal collective behavior, which depend only on the spatial dimension and symmetry of the system.

The dispersed cluster morphology of the amorphous metastable phase and the apparent exponential relaxation of the average cluster size are no doubt intimately linked to the confinement of the large spheres and the greatly reduced mobility of the larger clusters.[18] This limiting factor is relatively easy to model in the present phenomenological approach (which assumes a priori the existence of a transient steady state) since it is contained in the cluster mobility γ_i. The reversible nature of the depletion interaction and the reduced mobility of larger clusters would seem to be the dominant physical factors governing the formation of the observed steady-state morphology. An alternative approach would be one more conventional to spinodal decomposition and nucleation in binary fluids, with some type of macroscopic driving force linked to the free energy of the mixture. The limited mobility of the large-sphere clusters could then be modeled, for example, with an order-parameter dependent kinetic coefficient.

It is important to note, however, the limited role played by any interfacial tension between coexisting domains of large-sphere rich and large-sphere poor phases. In a sense, this reflects the kinetic arrest at a morphology that is really not macroscopic in nature but corresponds more to the earliest stages of segregation in a binary fluid. As such, an approach based on eq 1 seems particularly well suited. Under different quench conditions, the dense metastable fluid phase should grow via nucleation,[20] which is of practical relevance to such things as the promotion of crystallization in solutions of globular proteins.[21] One could envision using much smaller particles, for example, so that a crossover from aggregation-type behavior to surface-tension limited regimes of coarsening via spinodal decomposition and nucleation might be accessed. Experiments designed to address these differences will be carried out in the future.

Acknowledgment. The author is indebted to B.P. Lee for useful discussions regarding the theory of eq 1 and assistance with the cluster-tabulation code, R.K. Hobbie for assistance with the structure-factor code, and J.C. Crocker for advice on materials, sample cells and digital-video microscopy in general. Certain commercial materials are identified in this article in order to adequately specify the experimental procedure. Such identification does not imply recommendation or endorsement by the National Institute of Standards and Technology, nor does it imply that these materials are the best available for the purpose.

LA990397O

(19) Crocker, J. C.; Mateo, J. A.; Dinsmore, A. D.; Yodh, A. G. *Phys. Rev. Lett.* **1999**, *82*, 4352.

(20) (a) Evans, R. M. L.; Cates, M. E. *Phys. Rev. E* **1997**, *56*, 5738. (b) Evans, R. M. L.; Poon, W. C. K. *Phys. Rev. E* **1997**, *56*, 5748.

(21) ten Wolde, P. R.; Frenkel, D. *Science* **1997**, *277*, 1975.